

# Distinct and overlapping alterations in motor and sensory neurons in a mouse model of spinal muscular atrophy

Sibylle Jablonka<sup>1</sup>, Kathrin Karle<sup>1</sup>, Beatrice Sandner<sup>1</sup>, Catia Andreassi<sup>1,2</sup>, Katja von Au<sup>1,3</sup> and Michael Sendtner<sup>1,\*</sup>

<sup>1</sup>Institute for Clinical Neurobiology, Josef-Schneider-Str. 11, D-97080 Wuerzburg, Germany, <sup>2</sup>MRC LMCB, University College of London, Gower Street, WC1 6BT London, UK and <sup>3</sup>Department of Neuropediatrics, Charité University Medical School of Berlin, Augustenburger Platz 1, D-13353 Berlin, Germany

**Motor neuron degeneration is the predominant pathological feature of spinal muscular atrophy (SMA). In patients with severe forms of the disease, additional sensory abnormalities have been reported. However, it is not clear whether the loss of sensory neurons is a common feature in severe forms of the disease, how many neurons are lost and how loss of sensory neurons compares with motor neuron degeneration. We have analysed dorsal root ganglionic sensory neurons in *Smn*<sup>-/-</sup>; *SMN2* mice, a model of type I SMA. In contrast to lumbar motor neurons, no loss of sensory neurons in the L5 dorsal root ganglia is found at post-natal days 3–5 when these mice are severely paralyzed and die from motor defects. Survival of cultured sensory neurons in the presence of NGF and other neurotrophic factors is not reduced in comparison to wild-type controls. However, isolated sensory neurons have shorter neurites and smaller growth cones, and  $\beta$ -actin protein and  $\beta$ -actin mRNA are reduced in sensory neurite terminals. In footpads of *Smn*-deficient mouse embryos, sensory nerve terminals are smaller, suggesting that *Smn* deficiency reduces neurite outgrowth during embryogenesis. These data indicate that pathological alterations in severe forms of SMA are not restricted to motor neurons, but the defects in the sensory neurons are milder than those in the motor neurons.**

## INTRODUCTION

Autosomal recessive spinal muscular atrophy (SMA) is caused by the loss of the telomeric copy of the survival of motor neuron gene (*SMN1*) on human chromosome 5q13 (1). Despite the widespread expression of SMN in various tissues and neuronal cell types, motor neurons are predominantly affected, and motor neuron degeneration is the leading pathological alteration in this disease (2). The severity of the SMA phenotype is modified by the number of centromeric *SMN2* copies (3–5). In the most severe form of the disease (type I SMA) according to Munsat and Davies (6) and Roberts *et al.* (7), sensory defects have also been observed (8). In particular in type I SMA patients, reduced nerve conduction velocity has been recorded from mixed and sensory nerves (9), and severely affected SMA type I patients with congenital muscular hypotonia which progressed to early death showed inexcitability of sensory nerves (10). More

detailed analysis of sensory nerves from seven type I SMA patients revealed axonal degeneration in sural nerves (11). In type I SMA patients, many empty myelin sheaths and atrophic axons in the sensory nerves correlated with typical signs of sensory axonopathy in electrophysiological analyses. Interestingly, SMA II and SMA III patients did not show sensory nerve pathology.

On the basis of these findings, we analysed the loss of sensory neurons in the L5 dorsal root ganglia (DRGs) of post-natal *Smn*<sup>-/-</sup>; *SMN2* mice. These mice serve as a model for human type I SMA (12). We investigated dorsal root sensory neurons at different developmental periods. E14 was chosen to investigate defects in neurite outgrowth at a stage when sensory nerve fibres normally reach their target, the skin. Survival of sensory neurons was investigated at post-natal days 3–5, when the developmental period of physiological cell death is over and neuronal losses due to pathological processes become apparent. We also investigated

\*To whom correspondence should be addressed. Tel: +49 93120149771; Fax: +49 93120149788; Email: sendtner@mail.uni-wuerzburg.de

survival, neurite growth and growth cone morphology in cultured sensory neurons from E14 mouse embryos. Isolated sensory neurons from such embryos need trophic support to survive in cell culture, and neurite growth resembles initial fibre outgrowth and not a regenerative response resembling that of adult neurons after axotomy.

The number of cell bodies in the L5 dorsal root ganglia (DRGs) of *Smn*<sup>-/-</sup>; *SMN2* mice is not reduced at post-natal day 5, when these mice are severely paralyzed due to defects in motor neurons. The sensory nerve endings in the skin of 14-day-old *Smn*<sup>-/-</sup>; *SMN2* embryos appear smaller in comparison to controls. In isolated sensory neurons,  $\beta$ -actin mRNA and protein are reduced in distal neurites and growth cones. Growth cones of *Smn*-deficient cultured sensory neurons are smaller and their neurites are shorter. These findings suggest that sensory neurons are also affected by *Smn* deficiency, but the pathological changes are more discrete than those in motor neurons.

## RESULTS

### Quantification of neurons in L5 DRGs

Previous studies have shown that the number of spinal motor neurons is reduced in various models of SMA (12–15). Three-to-five-day-old *Smn*<sup>-/-</sup>; *SMN2* mice that serve as a model for type I SMA exhibit a 17% loss of motor neurons in the lumbar spinal cord (12). At that stage, these mice are severely paralyzed, and they normally do not survive longer than 5–7 days after birth. To investigate whether sensory neurons are also affected by the disease, we counted the number of neurons in L5 DRGs from *Smn*<sup>-/-</sup>; *SMN2* mice. *Smn*<sup>-/-</sup>; *SMN2* mice and age-matched controls were perfused at post-natal days 1, 3 and 5. The spinal cord together with the DRGs was dissected, and 15  $\mu$ m paraffin serial sections were prepared and Nissl stained. We counted the nuclei of neuronal cell bodies in every 10th section of the L5 DRGs (Fig. 1A). No significant difference was observed between *Smn*<sup>-/-</sup>; *SMN2* and control DRGs (Fig. 1B) at any stage, even at post-natal day 5 when the mice are severely paralyzed, indicating that survival of sensory neurons in *Smn*<sup>-/-</sup>; *SMN2* mice is not reduced when the motor neuron loss becomes apparent in this disease.

### Neurite growth is reduced in *Smn*-deficient sensory neurons

We then investigated whether reduced *Smn* levels influence neurite growth in sensory neurons at E14. Previous studies with isolated motor neurons from *Smn*<sup>-/-</sup>; *SMN2* mice (16) and a zebrafish model (17) in which *Smn* was repressed by Morpholino knockdown have shown that *Smn* deficiency leads to defects in neurite outgrowth in motor neurons. Lumbar DRGs contain various types of neurons, including proprioceptive, fast- and slow-conducting sensory neurons. These subpopulations differ in their response to different neurotrophic factors (NFs). NT-3 predominantly supports survival of proprioceptive neurons (18,19), whereas BDNF acts on neurons which are responsive to tactile stimuli (20,21). Nerve growth factor (NGF) predominantly supports small

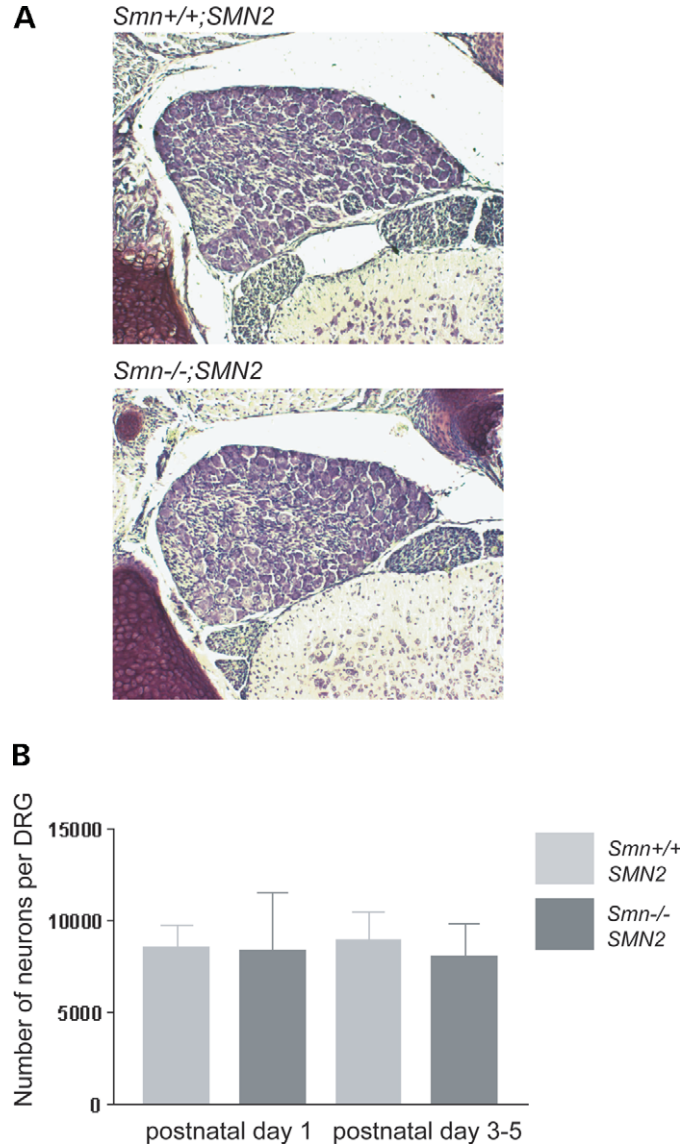


**Figure 1.** Quantification of neuronal cell bodies in L5 DRGs of *Smn*<sup>-/-</sup>; *SMN2* and *Smn*<sup>+/+</sup>; *SMN2* mice. Cell numbers were counted at post-natal days 1, 3 and 5 in sectioned L5 DRGs from *Smn*<sup>-/-</sup>; *SMN2* mice and age-matched controls (A). Neurons were counted in every 10th section. The counts are depicted as bar charts (B). No difference in cell number was observed between *Smn*<sup>-/-</sup>; *SMN2* (P1 *n* = 3; P3–5 *n* = 4; black) and controls (P1 *n* = 3; P3–5 *n* = 4; grey). Data represent mean  $\pm$  SD.

pain-conducting neurons (21), and GDNF acts more broadly on these different subtypes of neurons (19,22). Therefore, to investigate whether *Smn* deficiency differentially affects these subpopulations, NGF, GDNF, BDNF and NT-3 were separately added at a concentration of 10 ng/ml each as survival factors to the sensory neuronal cultures. In a first attempt, we investigated whether NGF, NT-3, BDNF and GDNF responsiveness is altered in *Smn*<sup>-/-</sup>; *SMN2* sensory neurons. Survival of DRG neurons did not differ in the presence of these different NFs (Fig. 2A and B). Without NFs, neurite outgrowth is normally very low (Fig. 2C), and there was no difference between neurite-bearing cells in mutants and controls (data not shown). We then investigated the size

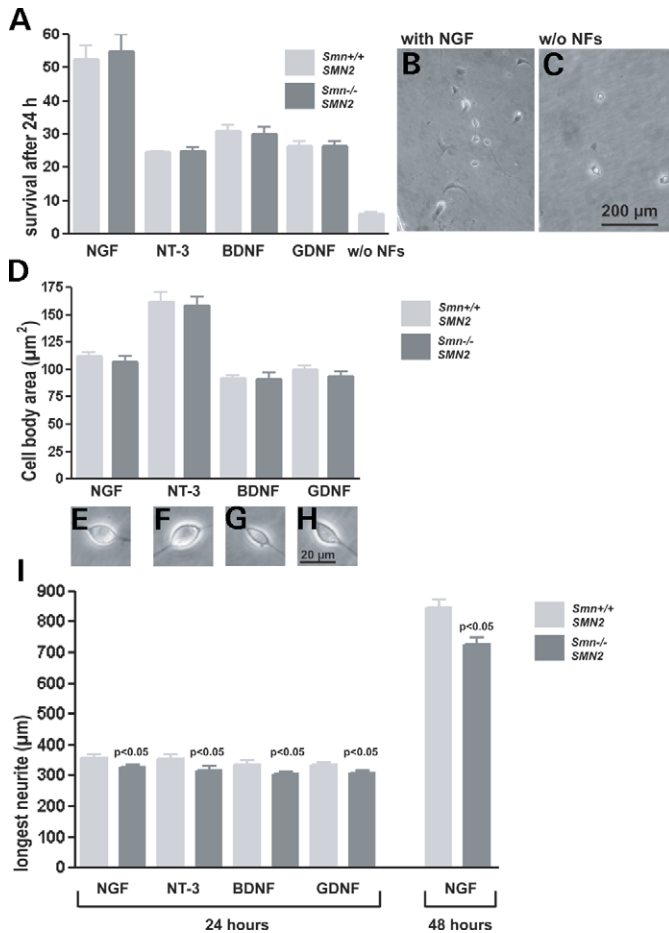


**Figure 2.** Survival, size of cell bodies and neurite length in cultured dorsal root ganglionic neurons from *Smn*<sup>-/-</sup>;*SMN2* and control embryos. Cells were cultured for 24 h in the presence of NGF, NT-3, BDNF and GDNF (10 ng/ml each) and for 48 h in the presence of NGF to support the survival of various sensory neuronal subtypes. Cells were counted immediately after plating and after 24 h. Survival of cells treated with different NFs and without NFs (A), morphology of NGF-treated cultures (B) and controls without NFs (C), cell body size (D) and morphology (E–H). No differences in cell survival and size of cell bodies were observed between *Smn*-deficient sensory neurons and controls. Neurite length was measured; data are shown as bar charts (I). After 24 h, neurites of *Smn*-deficient sensory neurons (black bar) are shorter than controls (grey bar) in the presence of NGF (–9%,  $P < 0.05$ ), NT-3 (–11%,  $P < 0.05$ ), BDNF (–8%,  $P < 0.05$ ) and GDNF (–7%,  $P < 0.05$ ). Neurite length reduction of *Smn*-deficient cells increases to 14% in the presence of NGF after 48 h of culturing (results from three independent experiments). Data represent mean  $\pm$  SEM.

of cell bodies in these different groups. Although the subpopulations of NT-3 responsive neurons showed larger cell bodies (Fig. 2D and F) both in mutant and in control cultures, no differences were observed between control and *Smn*<sup>-/-</sup>;*SMN2* sensory neurons.

To investigate neurite outgrowth, the cells were fixed with 4% paraformaldehyde (PFA) and immunostained with antibodies against phosphorylated Tau protein (red) and MAP-2 (green) after 24 h in culture (data not shown). The neuronal processes of *Smn*-deficient cells were slightly but significantly shorter when compared with wild-type controls (Fig. 2I). No

significant difference was observed with respect to the survival factor added to these cultures. More than 200 cells in three independent experiments were measured and the reduction was significant ( $P < 0.05$ ) for each group, as shown in Figure 2I. To investigate whether longer culture periods lead to normalization of neurite outgrowth, *Smn*<sup>-/-</sup>;*SMN2* sensory neurons were cultured with NGF for 48 h. The difference in neurite length between mutant and control cultures persisted, indicating that the effect of *Smn* deficiency cannot be explained by a delay of neurite growth that is compensated within 48 h.

### Subcellular distribution of *Smn*, hnRNP-R and $\beta$ -actin in cultured sensory and motor neurons

To investigate and compare the distribution of *Smn*, hnRNP-R and  $\beta$ -actin protein in sensory and motor neurons, both types of neurons were prepared from E14 embryos and taken into culture. Sensory neurons were plated on Laminin-111 (according to (23)) and cultured in the presence of 10 ng/ml NGF for 24 h. Motor neurons were grown on the same substrate for 7 days in the presence of BDNF and CNTF (10 ng/ml each). After fixation, sensory and motor neurons were stained with antibodies against *Smn*,  $\beta$ -actin and hnRNP-R, respectively. Staining against hnRNP-R was combined with antibodies against  $\beta$ -actin (Fig. 3A, E and I) and *Smn* (Fig. 3C, G and K) in motor and sensory neurons (Fig. 3B, F and J and D, H and L). The accumulation of hnRNP-R, *Smn* and  $\beta$ -actin in the distal part of motor axons was more pronounced in wild-type motor neurons than in wild-type sensory neurons (Fig. 3I and J and K and L, arrow).

### hnRNP-R and $\beta$ -actin distribution in neurites and growth cones of primary cultured sensory neurons

We have previously observed that *Smn*, hnRNP-R,  $\beta$ -actin and  $\beta$ -actin mRNA accumulation is reduced in axon terminals of cultured *Smn*-deficient motor neurons (16). Therefore, we investigated the distribution of these proteins in sensory neurons cultured from control and *Smn*-deficient mice. In addition, we compared the growth cone size of *Smn*-deficient and wild-type sensory neurites (Fig. 4). After 24 h in the presence of NT-3, BDNF, GDNF and NGF, the sensory neurons were fixed and stained with monoclonal antibodies against  $\beta$ -actin and hnRNP-R. hnRNP-R staining in growth cones of sensory neurons is restricted to the pars compacta (Fig. 4F, arrow). Growth cone size was significantly reduced in sensory neurons ( $P < 0.0001$ ) (Fig. 4M). Immunoreactivity of  $\beta$ -actin protein appeared highly reduced in the distal part of the neurites (Fig. 4D and L). No differences in growth cone size were observed in various subgroups of sensory neurons, which survive in the presence of NGF, NT-3, BDNF or GDNF (Fig. 4M).

### $\beta$ -Actin mRNA is reduced in growth cones of cultured sensory neurons from *Smn*-deficient embryos

On the basis of the finding that growth cones of *Smn*-deficient sensory neurons contain less  $\beta$ -actin immunoreactivity than wild-type controls, we investigated whether  $\beta$ -actin mRNA

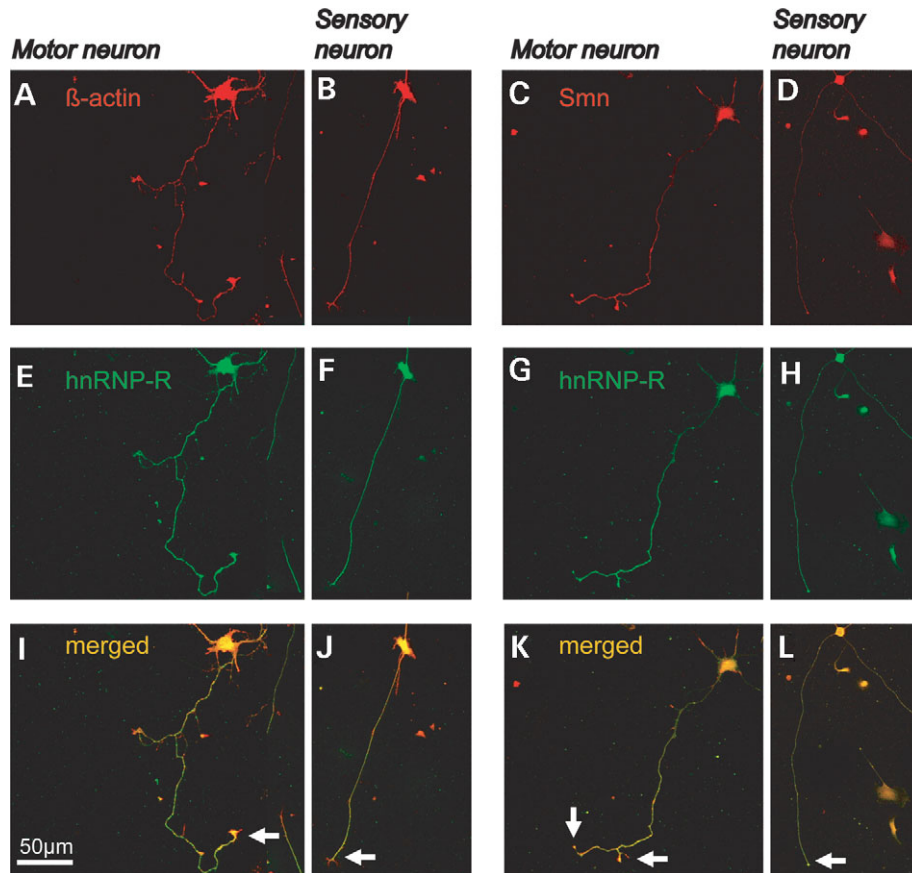


**Figure 3.** Smn, hnRNP-R and  $\beta$ -actin distribution in cultured sensory and motor neurons from Smn wild-type embryos. DRGs were isolated from 14-day-old Smn wild-type embryos and cultured for 24 h in the presence of NGF (10 ng/ml). The cells were then fixed with 4% PFA and stained with antibodies against hnRNP-R (green),  $\beta$ -actin and Smn (red). In parallel, motor neurons were isolated from the same mouse embryos and cultured for 7 days. In motor neurons, hnRNP-R,  $\beta$ -actin and Smn strongly accumulate in the distal part of the axon (A, C, E and G, arrows in I and K). In sensory neurons, the distribution of Smn, hnRNP-R and  $\beta$ -actin is similar, but the accumulation at the neuron terminal is less pronounced (B, D, F and H, arrows in J and L).

is also reduced. For this purpose, we performed *in situ* hybridization with an antisense probe against actin mRNA. Light microscopic analysis revealed a reduced signal for actin mRNA in the distal part of Smn-deficient sensory neurons (Fig. 5B and D) in contrast to wild-type cells (Fig. 5A and C). An actin mRNA sense probe was used as a negative control (Fig. 5E).

#### Morphological characterization of sensory nerve endings in footpads of Smn-deficient mice

The observation that Smn-deficient cultured sensory neurons do not show any alterations with respect to cell survival but exhibit defects in neurite elongation and reduced growth cone size prompted us to examine sensory nerve endings *in vivo* at a stage when these neurites grow out and make contact with their targets. For this purpose, we isolated footpads from E14 *Smn*<sup>-/-</sup>;*SMN2* embryos and control littermates. After fixation, 10  $\mu$ m thick cryosections were cut and stained with a polyclonal antibody against neurofilament-M. Sections were analysed under a confocal microscope for morphological alterations of the nerve endings in the epidermis of the footpads.

In comparison to controls (Fig. 6A and C), nerve endings from Smn-deficient embryos do not reach the outer epidermal layer (Fig. 6B and D). Higher magnification of innervating nerves revealed that sensory neuron endings were prominent in control embryos and showed a typical globe-like structure (Fig. 6E and F). In contrast, the nerve endings were much thinner in *Smn*<sup>-/-</sup>;*SMN2* embryos (Fig. 6G and H). We have also quantified the number of sensory nerve endings in *Smn*<sup>-/-</sup>;*SMN2* and controls. No difference was observed in the number of nerve endings per footpad (data not shown).

#### DISCUSSION

SMA is generally considered as a disease exclusively affecting motor neurons. Nevertheless, several clinical observations have been made with type I SMA patients that sensory neurons are also affected. Abnormal sensory conduction velocity has been reported (9–11), and analysis of sural nerve biopsies revealed various degrees of axonal degeneration (11). It is not known how generalized these effects are or whether the axonal loss observed in the nerve biopsy material

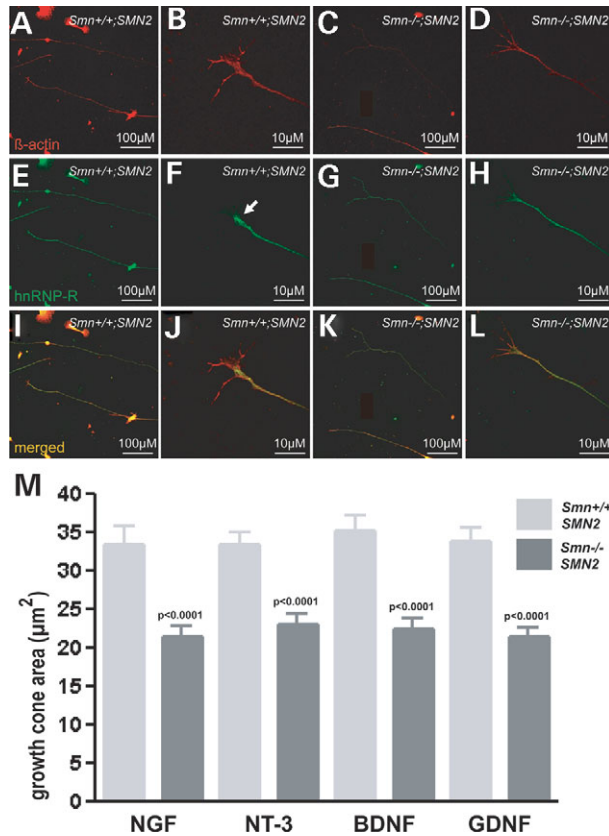


**Figure 4.** Reduced  $\beta$ -actin content in neurite terminals of isolated *Smn*-deficient sensory neurons. Dorsal root ganglionic sensory neurons from *Smn*<sup>-/-</sup>;SMN2 and *Smn*<sup>+/+</sup>;SMN2 embryos were cultured for 24 h, fixed with 4% PFA and stained with antibodies against  $\beta$ -actin (red) and hnRNP-R (green). HnRNP-R and  $\beta$ -actin are homogeneously distributed throughout the cell bodies and proximal neurites in wild-type (A, B, E, F, I and J) and *Smn*-mutant sensory neurons (C, D, G, H, K and L). Staining in the distal parts of *Smn*-deficient neurites appears weaker. The area of the growth cones of *Smn*-deficient sensory neurons (black bar) and wild-type controls (grey bar) treated with NT-3, NGF, BDNF and GDNF was determined by staining against  $\beta$ -actin (B, D, J and L), followed by morphological analysis (M). The growth cone area of *Smn*-deficient sensory neurons in the presence of each survival factor is significantly reduced ( $P < 0.0001$ ).

correlates with enhanced cell death of the corresponding sensory neurons in the DRGs.

We have analysed the number of sensory neurons in the L5 DRG and the morphology of sensory nerve terminals in the skin of *Smn*-deficient mouse embryos. Although no significant loss of sensory neurons was observed, sensory neurons from the severely affected SMA mouse model do not develop properly. Their terminals in the skin are much smaller at embryonic day 14. This correlates with defects in neurite growth and growth cone morphology in sensory neurons isolated from mouse embryos at the same developmental stage. Growth cones of these sensory neurons were significantly smaller in cultured *Smn*-deficient neurons. Accumulation of the *Smn* interaction partner hnRNP-R is less pronounced in the distal part of the sensory nerve processes. Moreover,  $\beta$ -actin protein and mRNA levels are reduced in growth cones of sensory neurites, indicating that similar pathophysiological

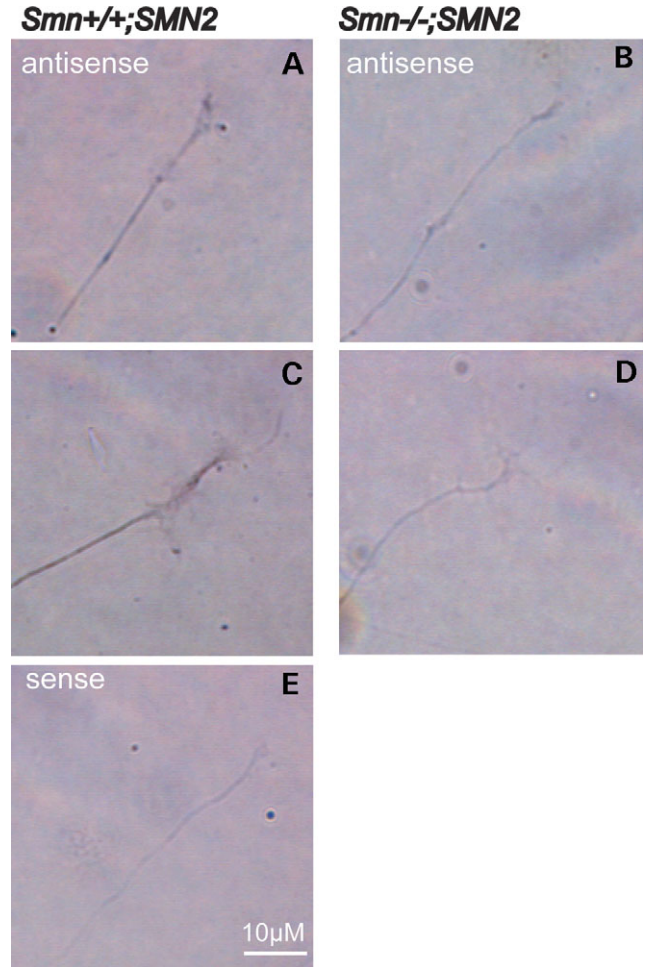


**Figure 5.** Reduction of actin mRNA in growth cones of *Smn*-deficient sensory neurons. *In situ* hybridization of cultured sensory neurons derived from *Smn*<sup>-/-</sup>;SMN2 (B and D) and *Smn*<sup>+/+</sup>;SMN2 mice with an antisense probe against actin mRNA (A and C). The signal for actin mRNA is reduced in the distal part of the neurites in *Smn*-deficient sensory neurons (B and D). An actin-sense probe was used as negative control and did not reveal a detectable signal (E).

processes as those observed in *Smn*-deficient motor neurons are responsible for these defects.

Sensory defects have so far only been reported in severe SMA, particularly in patients with pre-natal disease onset. For example, a patient described by Rudnik-Schoneborn *et al.* (11), who was ventilated from birth on with no motor function at all, showed a fibre density of 3500/mm<sup>2</sup> in the sural nerve, whereas age-matched controls have more than 20 000 fibres per mm<sup>2</sup>. This finding indicates that sensory defects develop early in severe SMA, at the same time when motor defects become apparent. Similarly, isolated sensory neurons from 14-day-old *Smn*<sup>-/-</sup>;SMN2 mouse embryos show reduced neurite growth, and the growth cones in the skin of these mice are smaller than in controls. Surprisingly, these alterations did not result in the loss of sensory cell bodies in the L5 DRG at post-natal days 3–5, indicating that reduced SMN levels do not affect survival of sensory neurons in culture or *in vivo*.

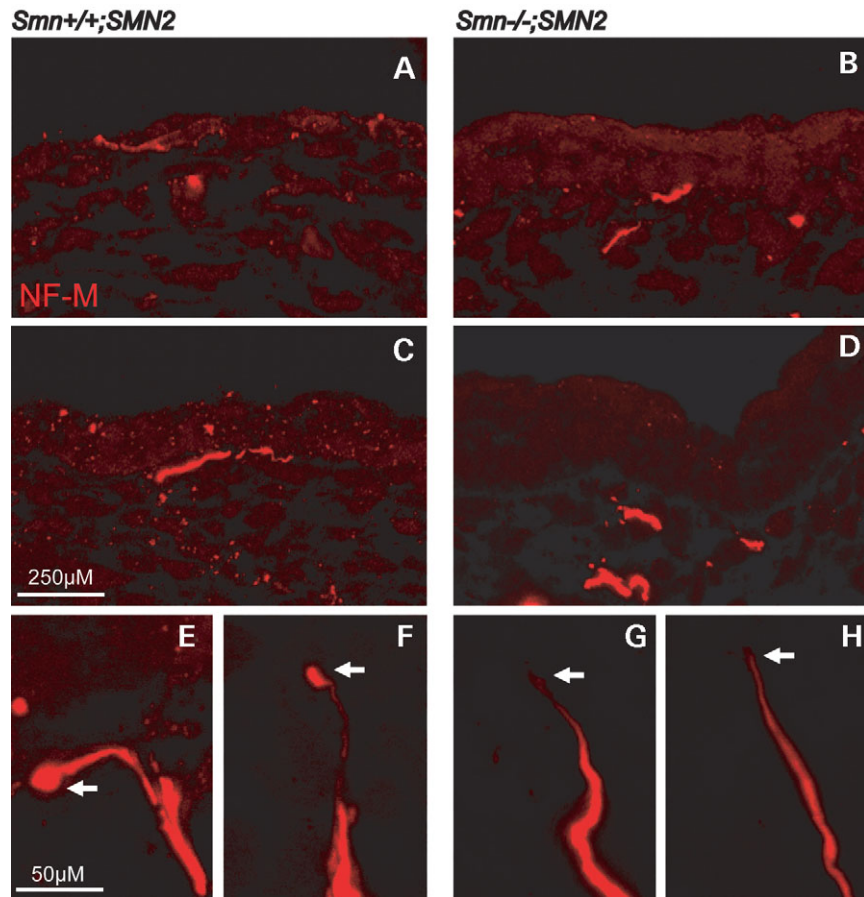


**Figure 6.** Nerve endings of sensory neurons in footpads from E14-old-*Smn*-deficient mouse embryos. Cryosections of footpads from *Smn*-wild-type and *Smn*-deficient E14 embryos were prepared. Each section was stained with a polyclonal antibody against neurofilament-M (red) and analysed by confocal microscope. Distal nerve endings from *Smn*-deficient sensory neurons do not reach the outer epidermal layer (**B** and **D**) in contrast to sensory nerve endings from control embryos (**A** and **C**). Nerve endings of sensory neurons from wild-type embryos were prominent, and the terminals showed a typical globe-like structure (**E** and **F**, arrow). In contrast, the nerve endings in *Smn*<sup>-/-</sup>;*SMN2* embryos were much thinner (**G** and **H**, arrow).

Interestingly, motor neuron loss in the same mice is small at birth and increases during the following 3–5 days (12). When motor neurons are isolated at E14, axon growth is reduced during a period of 7 days in culture. This indicates that axon pathology precedes neuronal cell death in motor neurons. Indeed, when isolated motor and sensory neurons are grown in culture in the presence of NFs, cell death is not enhanced, although the defects in neurite growth are clearly apparent under these *in vitro* conditions. This suggests that the cell death of motor neurons is a consequence of loss of contact and subsequent loss of trophic support from skeletal muscle. The finding that treatment with cardiotrophin-1, neurotrophic factor that is secreted from developing skeletal muscle to innervating motor neurons, can reduce motor neuron loss in *Smn*-deficient mice (24) supports this hypothesis.

The neurite growth defect observed with isolated sensory neurons is much less pronounced in comparison to motor neurons. Neurites from sensory neurons grow much faster than from isolated motor neurons under similar culture conditions. Within 24 h, they grow distances up to 300 or 400  $\mu\text{m}$ , whereas axons from cultured motor neurons need 7

days for the same distance. Growth of sensory and motor axons in cell culture differs by the frequency of growth cone collapses, changes in growth directions and turns, which are much more frequent in motor than in sensory axons (Fig. 3A and B). The growth cone plays an essential role in axon guidance (25), and  $\beta$ -actin dynamics regulate axon growth direction (26). The growth cone in isolated sensory neurons is smaller than in motor axons, and this reflects differences in neurite growth between these two types of cells. The finding that defects in motor axon guidance are a dominant feature after RNAi knockdown of *Smn* in zebrafish (17) is in line with this idea.

In summary, *Smn*<sup>-/-</sup>;*SMN2* mice exhibit specific alterations in sensory neurons, which are less prominent than defects in motor neurons. Neurites are shorter and growth cones are smaller in sensory neurons from *Smn*-deficient embryos. Reduced levels of  $\beta$ -actin mRNA and protein in sensory growth cones point to a similar pathomechanism in both cell types, indicating that *Smn* deficiency might result in more widespread changes in the nervous system, particularly in type I SMA.

## MATERIALS AND METHODS

### Quantification of neurons per DRG

Mice were deeply anaesthetized and transcardially perfused with 4% PFA at post-natal days 1, 3 and 5. The spinal cord with the attached DRGs was prepared, and 15  $\mu$ m paraffin serial sections were cut. Neurons in DRGs were counted in every 10th section from L5 spinal cord segments. The raw counts were corrected for double counting of split nucleoli, as described (27).

### Sensory neuronal culture from mouse embryos

L1 to L5 DRGs were dissected from E14 embryos in parallel with the ventral part of the spinal cord. The DRGs were transferred to phosphate-buffered saline (PBS) and incubated with trypsin (0.05% in HBSS) for 30 min. Trypsin digestion was stopped by the addition of F14 medium (Gibco) containing 10% horse serum and 35 mM KCl. The cell suspension was pre-plated for 3–4 h to suppress growth of non-neuronal cells. The supernatant was centrifuged (10 min at 400g), and the cell pellet was resuspended in F14 medium containing 10% horse serum and 35 mM KCl. The cells were counted and plated at 2000 cells per  $\text{cm}^2$  on polyornithine-coated plates on Laminin-111. The cells were incubated for 24 or 48 h, respectively, at 37°C and 5%  $\text{CO}_2$ .

### Immunocytochemistry and data analysis

Sensory neurons grown for 24 or 48 h on glass cover slips were fixed with 4% PFA. After treatment with 10% bovine serum albumin (BSA), the fixed cells were incubated O/N at +4°C with the following primary antibodies: rabbit antibodies against phospho-Tau (Sigma, 1  $\mu$ g/ml) and hnRNP-R [(28), 1:1000] and a monoclonal antibody against Smn (Transduction Laboratories, 1:1000),  $\beta$ -actin (Abcam, 1:1000) and Map-2 (Sigma, 1:1000). Cells were then washed three times with Tris-buffered saline (TBS)-T and incubated for 1 h at room temperature with Cy2- and Cy3-conjugated secondary antibodies (Dianova, 1:200). After washing with TBS-T, cover slips were embedded in Mowiol. For the quantification of neurite length and growth cone area, phospho-Tau-positive processes and  $\beta$ -actin-positive growth cones were scored. Images recorded at the confocal microscope (Leica) were analysed using the Scion Image software package. Data were analysed using the Student's *t*-test for significance of differences.

### In situ hybridization

Cells grown on glass cover slips were fixed with 4% PFA in PBS for 15 min at room temperature and then washed with PBS containing 0.1% active DEPC for 10 min at room temperature. Cells were then permeabilized with 0.3% (v/v) Triton in PBS for 20 min at room temperature, and endogenous peroxidase activity was quenched through incubation in 0.3% (v/v)  $\text{H}_2\text{O}_2$  in methanol for 40 min at room temperature. Following a wash in 5 $\times$  SSC, cover slips were pre-incubated in hybridization buffer [4 $\times$  SSC, 20% dextran sulphate, 50% formamide, 0.25 mg/ml poly(A), 0.25 mg/ml salmon sperm DNA, 0.25 mg/ml tRNA, 0.1 M dithiothreitol (DTT),

0.5 $\times$  Denhardt's] for 1 h at 37°C. Then, fresh hybridization solution containing 3' biotinylated sense or antisense actin oligonucleotide (200 ng/ml, GeneDetect) was applied to the cover slips at 200 ng/ml. Hybridization was carried out for 24 h at 37°C. Two low stringency washes in 1 $\times$  SSC, 10 mM DTT were performed for 15 min at 55°C and followed by two washes in 0.5 $\times$  SSC, 10 mM DTT for 15 min at 55°C. Finally, a wash in 0.1 $\times$  SSC, 10 mM DTT for 10 min at 55°C was performed. A hybridized probe was detected through DAKO GenPoint, a Tyramide Signal Amplification System for *in situ* hybridization with biotinylated probes (DAKO), following the manufacturer's instruction. Finally, cover slips were counterstained with haematoxylin, dehydrated and mounted with Vitro-clud (Legenbrick). Images were acquired with an Axiophot microscope (Zeiss) equipped with a CCD camera using Axioplan 2 Software (Zeiss).

### Cryosections and NF-M antibody stainings of footpads from E14 embryos

Distal limbs from E14 embryos were prepared and frozen in Tissue-Tek. Cross-sections (10  $\mu$ m) from the footpad area were cut, mounted on gelatine-coated glass slides and pre-incubated with 10% BSA in 1 $\times$  TBS-T. After BSA treatment, the neurofilament-M antibody (Abcam, 1:200) staining was performed O/N. Sections were washed three times with TBS-T and incubated for 1 h at room temperature with Cy3-conjugated secondary antibodies (Dianova, 1:200). After washing with TBS-T, cover slips were embedded in DABCO. Images were recorded with a confocal microscope (Leica).

## ACKNOWLEDGEMENTS

We thank Christine Schneider for skilful technical assistance. This work was supported by grants from DFG, SFB 581, TP B1, the EU through the APOPIS project, the SMA Foundation and the Schilling Stiftung.

*Conflict of Interest statement.* None declared.

## REFERENCES

- Lefebvre, S., Burglen, L., Reboullet, S., Clermont, O., Burlet, P., Viollet, L., Benichou, B., Cruaud, C., Millasseau, P., Zeviani, M. *et al.* (1995) Identification and characterization of a spinal muscular atrophy-determining gene. *Cell*, **80**, 155–165.
- Crawford, T.O. and Pardo, C.A. (1996) The neurobiology of childhood spinal muscular atrophy. *Neurobiol. Dis.*, **3**, 97–110.
- Lefebvre, S., Burlet, P., Liu, Q., Bertrand, S., Clermont, O., Munnich, A., Dreyfuss, G. and Melki, J. (1997) Correlation between severity and SMN protein level in spinal muscular atrophy. *Nat. Genet.*, **16**, 265–269.
- Lorson, C.L., Hahnen, E., Androphy, E.J. and Wirth, B. (1999) A single nucleotide in the SMN gene regulates splicing and is responsible for spinal muscular atrophy. *Proc. Natl Acad. Sci. USA*, **96**, 6307–6311.
- Monani, U.R., Lorson, C.L., Parsons, D.W., Prior, T.W., Androphy, E.J., Burghes, A.H. and McPherson, J.D. (1999) A single nucleotide difference that alters splicing patterns distinguishes the SMA gene SMN1 from the copy gene SMN2. *Hum. Mol. Genet.*, **8**, 1177–1183.
- Munsat, T.L. and Davies, K.E. (1992) International SMA consortium meeting (26–28 June 1992, Bonn, Germany). *Neuromuscul. Disord.*, **2**, 423–428.
- Roberts, D.F., Chavez, J. and Court, S.D. (1970) The genetic component in child mortality. *Arch. Dis. Child*, **45**, 33–38.

8. Korinthenberg, R., Sauer, M., Ketelsen, U.P., Hanemann, C.O., Stoll, G., Graf, M., Baborie, A., Volk, B., Wirth, B., Rudnik-Schoneborn, S. and Zerres, K. (1997) Congenital axonal neuropathy caused by deletions in the spinal muscular atrophy region. *Ann. Neurol.*, **42**, 364–368.
9. Anagnostou, E., Miller, S.P., Guiot, M.C., Karpati, G., Simard, L., Dilenge, M.E. and Shevell, M.I. (2005) Type I spinal muscular atrophy can mimic sensory-motor axonal neuropathy. *J. Child Neurol.*, **20**, 147–150.
10. Omran, H., Ketelsen, U.P., Heinen, F., Sauer, M., Rudnik-Schoneborn, S., Wirth, B., Zerres, K., Kratzer, W. and Korinthenberg, R. (1998) Axonal neuropathy and predominance of type II myofibers in infantile spinal muscular atrophy. *J. Child Neurol.*, **13**, 327–331.
11. Rudnik-Schoneborn, S., Goebel, H.H., Schlote, W., Molaian, S., Omran, H., Ketelsen, U., Korinthenberg, R., Wenzel, D., Lauffer, H., Kreiss-Nachtshelm, M., Wirth, B. and Zerres, K. (2003) Classical infantile spinal muscular atrophy with SMN deficiency causes sensory neuronopathy. *Neurology*, **60**, 983–987.
12. Monani, U.R., Sendtner, M., Coovert, D.D., Parsons, D.W., Andreassi, C., Le, T.T., Jablonka, S., Schrank, B., Rossoll, W., Prior, T.W., Morris, G.E. and Burghes, A.H. (2000) The human centromeric survival motor neuron gene (SMN2) rescues embryonic lethality in *Smn*(<sup>-/-</sup>) mice and results in a mouse with spinal muscular atrophy (in process citation). *Hum. Mol. Genet.*, **9**, 333–339.
13. Frugier, T., Tiziano, F.D., Cifuentes-Diaz, C., Miniou, P., Roblot, N., Dierich, A., Le Meur, M. and Melki, J. (2000) Nuclear targeting defect of SMN lacking the C-terminus in a mouse model of spinal muscular atrophy. *Hum. Mol. Genet.*, **9**, 849–858.
14. Jablonka, S., Schrank, B., Kralewski, M., Rossoll, W. and Sendtner, M. (2000) Reduced survival motor neuron (*Smn*) gene dose in mice leads to motor neuron degeneration: an animal model for spinal muscular atrophy type III. *Hum. Mol. Genet.*, **9**, 341–346.
15. Hsieh-Li, H.M., Chang, J.G., Jong, Y.J., Wu, M.H., Wang, N.M., Tsai, C.H. and Li, H. (2000) A mouse model for spinal muscular atrophy. *Nat. Genet.*, **24**, 66–70.
16. Rossoll, W., Jablonka, S., Andreassi, C., Kroning, A.K., Karle, K., Monani, U.R. and Sendtner, M. (2003) *Smn*, the spinal muscular atrophy-determining gene product, modulates axon growth and localization of beta-actin mRNA in growth cones of motoneurons. *J. Cell Biol.*, **163**, 801–812.
17. McWhorter, M.L., Monani, U.R., Burghes, A.H. and Beattie, C.E. (2003) Knockdown of the survival motor neuron (*Smn*) protein in zebrafish causes defects in motor axon outgrowth and pathfinding. *J. Cell Biol.*, **162**, 919–932.
18. Wright, D.E., Zhou, L., Kucera, J. and Snider, W.D. (1997) Introduction of a neurotrophin-3 transgene into muscle selectively rescues proprioceptive neurons in mice lacking endogenous neurotrophin-3. *Neuron*, **19**, 503–517.
19. Baudet, C., Mikaelis, A., Westphal, H., Johansen, J., Johansen, T.E. and Ernfors, P. (2000) Positive and negative interactions of GDNF, NTN and ART in developing sensory neuron subpopulations, and their collaboration with neurotrophins. *Development*, **127**, 4335–4344.
20. Carroll, P., Lewin, G.R., Koltzenburg, M., Toyka, K.V. and Thoenen, H. (1998) A role for BDNF in mechanosensation. *Nat. Neurosci.*, **1**, 42–46.
21. Lewin, G.R., Ritter, A.M. and Mendell, L.M. (1992) On the role of nerve growth factor in the development of myelinated nociceptors. *J. Neurosci.*, **12**, 1896–1905.
22. Matheson, C.R., Carnahan, J., Urich, J.L., Bocangel, D., Zhang, T.J. and Yan, Q. (1997) Glial cell line-derived neurotrophic factor (GDNF) is a neurotrophic factor for sensory neurons: comparison with the effects of the neurotrophins. *J. Neurobiol.*, **32**, 22–32.
23. Aumailley, M., Bruckner-Tuderman, L., Carter, W.G., Deutzmann, R., Edgar, D., Ekblom, P., Engel, J., Engvall, E., Hohenester, E., Jones, J.C. et al. (2005) A simplified laminin nomenclature. *Matrix Biol.*, **24**, 326–332.
24. Lesbordes, J.C., Cifuentes-Diaz, C., Miroglio, A., Joshi, V., Bordet, T., Kahn, A. and Melki, J. (2003) Therapeutic benefits of cardiotrophin-1 gene transfer in a mouse model of spinal muscular atrophy. *Hum. Mol. Genet.*, **12**, 1233–1239.
25. Gundersen, R.W. and Barrett, J.H. (1980) Characterization of the turning response of dorsal root neurites towards nerve growth factor. *J. Cell Biol.*, **87**, 546–554.
26. Challacombe, J.F., Snow, D.M. and Letourneau, P.C. (1996) Actin filament bundles are required for microtubule reorientation during growth cone turning to avoid an inhibitory guidance cue. *J. Cell Sci.*, **109**, 2031–2040.
27. Masu, Y., Wolf, E., Holtmann, B., Sendtner, M., Brem, G. and Thoenen, H. (1993) Disruption of the CNTF gene results in motor neuron degeneration. *Nature*, **365**, 27–32.
28. Rossoll, W., Kroning, A.K., Ohndorf, U.M., Steegborn, C., Jablonka, S. and Sendtner, M. (2002) Specific interaction of *Smn*, the spinal muscular atrophy determining gene product, with hnRNP-R and *gry*-rbp/hnRNP-Q: a role for *Smn* in RNA processing in motor axons? *Hum. Mol. Genet.*, **11**, 93–105.